CHEMISTRY
A European Journal

A Journal of
ChemPubSoc Europe

Accepted Article

Title: Direct Immunoassay for Facile and Sensitive Detection of Small Molecule Aflatoxin B1 based on Nanobody

Authors: Yanfei Shen, Deng Pan, Guanghui Li, Huizhen Hu, Huaijia Xue, Mingming Zhang, Min Zhu, Xue Gong, Yuanjian Zhang, and Yakun Wan

To be cited as: *Chem. Eur. J.* 10.1002/chem.201801202

Link to VoR: http://dx.doi.org/10.1002/chem.201801202

Supported by
ACES

WILEY-VCH

10.1002/chem.201801202

WILEY-VCH

FULL PAPER

Direct Immunoassay for Facile and Sensitive Detection of Small Molecule Aflatoxin B_1 based on Nanobody

Deng Pan,[a], † Guanghui Li,[b], † Huizhen Hu,[a], † Huaijia Xue,[a] Mingming Zhang,[a] Min Zhu,[b] Xue Gong,[a] Yuanjian Zhang,[a] Yakun Wan*[b] and Yanfei Shen*[a]

Abstract: Aflatoxin B_1 (AFB_1), one of the most toxic mycotoxins, is classified as a group I carcinogen and ubiquitous in various foods and agriproducts. Thus, accurate and sensitive determination of AFB_1 is of great significance to meet the criteria of food safety. Direct detection of AFB_1 is difficult by monoclonal antibody (mAb) with large molecular size (~150 kD) since the target is too small to produce a detectable signal change. Herein, by combining the electrochemical properties of nanomaterials and the advantages of nanobodies, we developed a direct, highly selective and sensitive electrochemical immunosensor for small molecule detection. The proposed immunosensor had a wide calibration range of 0.01 to 100 $ng \cdot mL^{-1}$ and a low detection limit of 3.3 $pg \cdot mL^{-1}$ (*S*/*N*=3). Compared with the immunosensor prepared with mAb which was applied in the typical indirect immunoassay, the immunosensor in this work possessed 2 orders of magnitudes wider linear range and 10-fold more sensitivity. The as-obtained immunosensor was further successfully applied for sensing AFB_1 in real samples. This proposed assay would provide a simple, highly sensitive and selective approach for the direct immunoassay of small molecule AFB_1, and is extendable to the development of direct immunosensing systems for other small molecules detection by coupling nanocarbon and nanobody.

Introduction

With the improvement of the living conditions, food safety becomes one of the most important worldwide issues, in which the food pollution caused by mycotoxins is one important branch.[1] Aflatoxin is one of the most toxic mycotoxins produced by certain molds (Aspergillus flavus and Aspergillus parasiticus) and widely present in various food and agricultural products due to improper storage.[2] Among more than 20 identified aflatoxins, Aflatoxin B_1 (AFB_1) is the most toxic, and was listed as group I carcinogen by the International Agency for Research on Cancer. [3] Exposure to AFB_1 may cause mutagenesis, carcinogenesis and teratogenesis in human beings and animals, and even could cause human and animal acute poisoning death.[4] The increasing awareness and the intensifying legislative framework about AFB_1 worldwide has aroused the requirement for efficient analytical methods capable of simple, rapid and sensitive detection.

Currently, many chromatography-based analytical techniques have been developed as a standard method for the determination of AFB_1, including high-performance liquid chromatography (HPLC), and high-performance liquid chromatography-tandem mass spectrometry (HPLC-MS), which are sensitive and accurate. However, these methods typically require well-equipped laboratory facilities, time-consuming sample pretreatment and skilled operators, which significantly limit the applications for fast-screening of large amounts of practical samples.

Immunoassay, such as enzyme-linked immunosorbent assay (ELISA), has received increasing interest in the field of clinical diagnose and environmental monitoring due to the specific interaction between the antigen and its antibody.[5] However, direct non-competitive detection of small molecules such as AFB_1 is not sensitive enough by conventional antibody with large molecular size (~150 kD) since the target is too small to produce a detectable signal change. For this, an indirect competitive immunoassay is usually applied by utilizing a competing antigen to compete with the target AFB_1 for binding with an anti-AFB_1 monoclonal antibody. Typically, for AFB_1 immunoassay, the competing antigen could be obtained by conjugating standard AFB_1 with a carrier protein such as bovine serum albumin (AFB_1-BSA).[6] Thus, a direct non-competitive assay for AFB_1 becomes an interesting way to simplify the assay and increase the sensitivity.[2] However, there is still of great challenges to develop direct non-competitive immunoassay for small molecules (i.e., AFB_1) with conventional antibodies.

Recently, nanobody (Nb), the variable domain of heavy-chain-only antibodies found in camelids, which are able to bind selectively to a specific antigen, has attracted progressively growing interest in various fields such as drug exploitation and diagnosis.[7] Compared with common antibodies, the molecular size of Nbs is much smaller (12~15 kD, only around 1/10 of those of conventional antibodies). Furthermore, Nbs possess other great advantages such as good solubility, excellent affinities and specificity, high thermal stability and acid resistance, and ease of crossing the blood-brain barrier. However, the immunoassay of small molecules via Nbs has been rarely reported.[6c,8] Here, we fabricated an electrochemical immunosensor for the direct sensitive determination of small molecule AFB_1 by coupling the Nb and carbon nanomaterials without the use of competing antigens (see Figure 1).

[a] Dr. D. Pan, H. Z. Hu, M. M. Zhang, H. J. Xue, Dr. X. Gong, Prof. Y. J. Zhang, Prof. Y. F. Shen
Medical School, School of Chemistry and Chemical Engineering, Southeast University, 210009 Nanjing (China)
E-mail: Yanfei.Shen@seu.edu.cn
[b] Dr.G. H. Li, Dr. M. Zhu, Prof.Y. K. Wan
Shanghai Novamab Biopharmaceuticals Co., Ltd., 201203 Shanghai (China)
E-mail: ykwan@novamab.com
† D. Pan, H. Hu and G. Li contributed equally.

Supporting information for this article is given via a link at the end of the document.

10.1002/chem.201801202

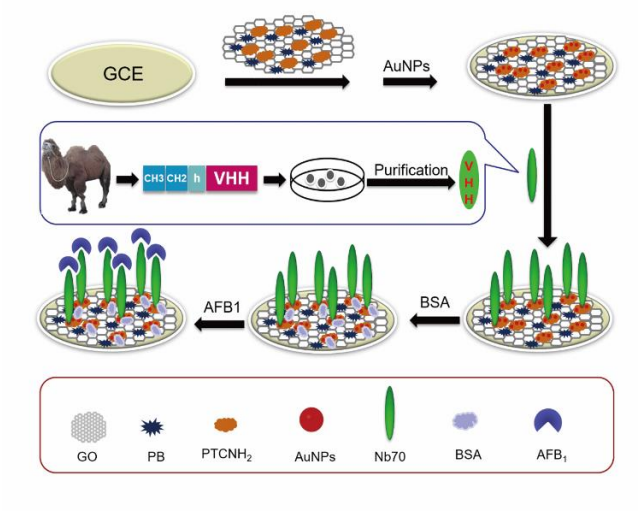

Figure 1. General fabrication procedure of the AFB_1 immunosensor.

Results and Discussion

Phage display technique was applied for the AFB_1-specific Nb isolation. 18 positive colonies were identified as the positive colonies, and their sequences were analysed. According to the diversity of amino acid sequences in complementarity determining region (CDR)3, these 18 Nbs were classified into three family (Figure S1a), named Nb30, Nb33, and Nb70, respectively. The selected Nbs were expressed and purified with Ni-NTA affinity columns and detected with SDS-PAGE. As shown in Figure S1b, the size of the Nbs are ~15 kDa, which is consistent with theoretical value, and with high quality of > 90% purity. The yields and other characters of the soluble Nbs were demonstrated in Figure S1c. As a result, Nb70 was chosen for the further research because of the brilliant yields.

Temperature is a vital factor to the activity and function of antibody. Therefore, thermal stability of Nb70 was evaluated. As a control experiment, the thermal stability of anti-AFB_1 monoclonal antibody (mAb), which was usually used in the indirect immunoassay of AFB_1, was also assessed. Both Nb70 and mAb were incubated at 20 °C, 50 °C, 65 °C, 80 °C and 95 °C in a thermo-controlled water bath for 10 min. Afterwards, the binding activity of the above samples to AFB_1-BSA was measured by ELISA (BSA protein as control). As shown in Figure 2a, mAb gradually lost binding ability by increasing temperature while the Nb70 show good thermal stability even at temperature as high as 95 °C. Besides, the samples were also evaluated by heating to 90 °C for various time (10, 20, 30, 40, 50, 60 min) (Figure 2b). The results demonstrated that even being incubated at 90 °C for 60 min, Nb70 also kept 80% activity, while the activity of mAb lost sharply after the treatment at 90 °C, and eventually kept 20% activity.

Antibody with high tolerance to organic solvents is of practical importance during real sample analysis, especially for lipophilic analytes. Aflatoxin, which is highly lipophilic, methanol (MeOH), acetone, ethanol (EtOH) and dimethylsulfoxide (DMSO) was applied during extraction. Therefore, the tolerance to organic solvents of Nb70 and commercial mAb was investigated by evaluating the binding activity after the addition of MeOH, acetone, EtOH and DMSO to the Nb70/Phosphate buffer solution (PBS) and mAb/PBS solution, with the final volume ratio of each organic solvent to total solution ranged from 10% to 50%. As a result, the relative activity decreased with the increase of organic solvent amount. It should be noted that, compared to mAb, Nb70 showed better tolerance than mAb to most of organic solvents, which maintained more than 80% of the binding activity in all solvents (Figure 3c-3f). However, the binding activity of mAb lost rapidly in presence of large amounts of MeOH (Figure 2c), Acetone (Figure 2d) and DMSO (Figure 2f), while EtOH showed less influence on the binding activity of mAb (Figure 2e). Therefore, Nb70 not only exhibited higher thermal stability, but also showed better tolerance to organic solvents than mAb, showing great potential for further application of biosensor development.

PB is typically used as an efficient mediator in electrochemical sensing system due to its excellent electrochemical properties Moreover, PB-based materials possess other advantages such as facile synthetic procedure, nontoxicity and low cost, which provides the possibilities for large-scale production and wide applications. However, the hydrolysis of PB results in the signal decrease of the PB-based electrochemical sensors, which limits its practical utilizations.[9] In order to improve the stability of PB, anchoring onto matrix is an efficient strategy. GO has been widely used as an efficient nanocarrier of nanoparticles for high loading to enhance the performance of biosensor due to its large specific surface area.[10] On the other hand, due to large amounts of charged functional groups on the GO surface, PB can be confined on GO by electrostatic attraction for the formation of GO-PB nanocomposite, which will in turn increase the water dispersibility

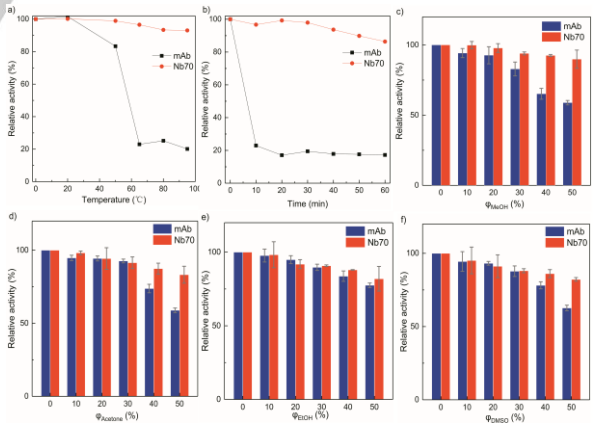

Figure 2. Thermo-sensitive and solvent durability analysis of Nb70 and mAb. Nb70 and mAb were diluted to 5 μg/mL in PBS and treated at a series of temperature (20 ˚C, 50˚C, 65˚C, 80 ˚C and 95˚C) for 10 min (a) and at 90 ˚C for 10 min, 20 min, 30 min, 40 min, 50 min and 60 min (b). Nb70 and mAb were mixed with equal volume of MeOH (c), Acetone (d), EtOH (e) and DMSO (f) and the volume fraction of organic solvents were 10%, 20%, 30%, 40% and 50% respectively. The binding abilities of Nb70 and mAb were tested by ELISA. Mean values and standard deviations were obtained from triplicate.

10.1002/chem.201801202

of PB.[11] Nevertheless, the relatively poor conductivity of GO-PB nanocomposite usually affects the sensitivity of electrochemical biosensors. For this, AuNPs were assembled with GO-PB as signal enhancers for higher electron conductivity and higher antibodies loading by using $PTCNH_2$, a derivative of PTCDA, as a linker between GO-PB and AuNPs, where $PTCNH_2$ can be conjugated with GO via the π-π stacking interaction, and provide plenty of amino groups for AuNPs anchoring and high conductivity for electrochemical sensing.[12]

As shown in the Figure 3a, SEM image of GO-PB assembly showed that PB was uniformly dispersed on the surface of GO (Figure 3a). The successful fabrication of GO-PB-$PTCNH_2$ was confirmed by UV-Vis spectra. As shown in Figure 3b, the spectrum of PB was dominated by the charge-transfer band of the mixed valence $Fe^{III}HCFe^{II}$ sequence with a maximum absorption at 723 nm.[13] A blue-shift up to 43 nm was observed for that of GO-PB, indicating an electron transfer between GO and PB. For the absorption of $PTCNH_2$, three characteristic absorption peaks were observed in the range of 420 nm to 700 nm due to the π-π* transition of the perylene moiety (Figure 3c).[12a] After the assembly of $PTCNH_2$ with GO-PB, the absorption increased at 500 nm but decreased at 583 nm and 632 nm (Figure 3c), confirming the interaction between $PTCNH_2$ and GO, which may be attributed to the π-π* interaction between the perylene moiety of $PTCNH_2$ and backbone of GO.[14] Thus UV-Vis spectra suggested the successful synthesis of the GO-PB-$PTCNH_2$ nanocomposite, which was supposed to serve as both an electrochemical probe and a substrate for further coupling biomolecules.

The stepwise fabrication processes of the immunosensor were monitored by CV measurements employing the $[Fe(CN)_6]^{3-}$ as a redox probe (Figure 4a). The CV of bare glassy carbon electrode (GCE) exhibited a pair of well-defined redox peaks with a peak-to-peak potential difference of less than 70 mV, indicating a reversible electrochemical process. The GCE was then coated with GO-PB-$PTCNH_2$ assembly followed by a coating of AuNPs. Interestingly, the peak current conversely increased, indicating that the GO-PB-$PTCNH_2$-AuNPs nanocomposite promoted the electron transfer of $[Fe(CN)_6]^{3-}$ at the electrode surface, which could be attributed to the enhanced electron transfer activity of the nanocomposite, as indicated by the UV-vis analysis in Figure 3. After the Nb70, BSA and AFB_1 were subsequently assembled onto the GCE, the peak current decreased gradually due to the increased resistance, which demonstrated the successful fabrication of the immunosensor.

Under the optimized detection conditions (Figure S2), the DPV measurements were applied to quantitatively assess the performance of the AFB_1 immunosensor. As shown in Figure 4b, the DPV currents decreased gradually with the increase of the AFB_1 concentration upon the assembly of AFB_1. By analyzing the relationship between the DPV currents decrease (Δ*I*) and the concentrations of AFB_1, it was found that Δ*I* displayed a good linear relationship with the logarithm of AFB_1 concentration in the range of 0.01-100 ng·mL^{-1} (Figure 4c, red). The corresponding regression equation could be expressed as Δ*I* (μA) = 0.537 lg*C* (pg·mL^{-1}) - 0.406, with a correlation coefficient of R^2=0.996, and the limit of detection (LOD, *S/N* = 3) was estimated to be 3.3 pg·mL^{-1}.

Meanwhile, as a control, the conventional anti-AFB_1 mAb, which was usually applied for the indirect immunoassay of AFB_1 by aid of the competing antigen AFB_1-BSA, was also used for the quantitative analysis of AFB_1 (Figure 4c, black). The DPV current change also increased with the improvement of the AFB1 concentration with a regression equation of Δ*I* (μA) = 0.165 lg*C* (pg·mL^{-1}) + 0.652. Of note, the biosensor using mAb instead of Nb70 exhibited a dynamic linear range (from 0.1 to 30 ng·mL^{-1}) of two orders of magnitudes narrower than that one by using Nb70. Moreover, the biosensor using mAb possessed a higher LOD (33.3 pg·mL^{-1}) and smaller slope (Figure 4c). That is, AFB_1 with the same concentration can cause much higher current change of the biosensor when using Nb70 instead of mAb. Therefore, the performance of the immunosensor using nanobody was superior than that of the mAb-based immunosensor.

In addition, the performance of the present immunosensor was also superior to those in previous reports even with indirect

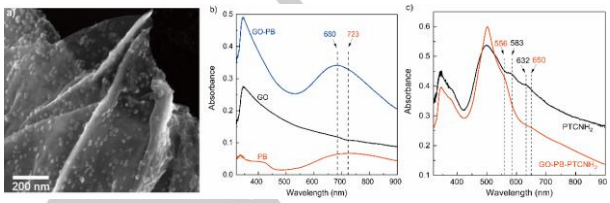

Figure 3. SEM image of GO-PB nanocomposite (a), and UV-Vis spectra of GO, PB and GO-PB (b), $PTCNH_2$ and GO-PB-$PTCNH_2$ (c).

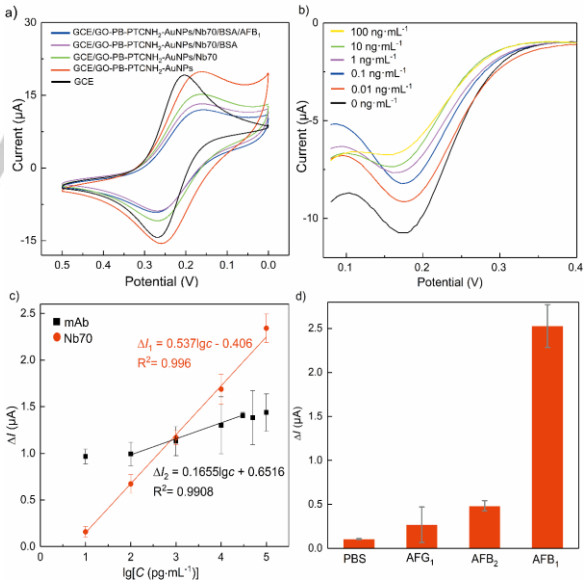

Figure 4. (a) Cyclic voltammograms of the modified GCE in 0.1 M PBS containing 2 mM $K_3[Fe(CN)_6]$ during each step of the immunosensor construction, scan rate of 100 mV·s^{-1}. (b) DPVs curves of the immunosensor with different concentrations of AFB_1. (c) The calibration curves of the Nb70 and mAb with different concentrations of AFB_1. (d) DPV peak currents of the immunosensor for PBS, and AFG_1, AFB_2 and AFB_1 with a concentration of 100 ng·mL^{-1} in PBS solution.

10.1002/chem.201801202

Table 1. Comparison of different methods for the detection of AFB_1.

Entry	Methods	Linear range ($ng \cdot mL^{-1}$)	LOD ($ng \cdot mL^{-1}$)	References
1	Electrochemical immunosensor	0.01-100	0.0033	This work
2	Label-free immunosensor	0.1-30	0.06	[15]
3	optical biosensor	0.5-20	0.16	[16]
4	HPLC[a]	5-35	0.06	[17]
5	Photoelectrochemical immunoassay	0.01-20	0.0021	[5]
6	Aptamer-based dipstick assay	0.1-10	0.1	[18]
7	Chemiluminescence	312.3-5214.9	46	[19]
8	Fluorescence immunoassay	0.01-5	0.008	[20]
9	Enzyme immunoassay	10-50	2	[21]
10	ICA[c]	—	0.25	[22]

[a] HPLC: High performance liquid chromatography, [b] LC-MS/MS: Liquid Chromatography-Tandem Mass Spectrometry, [c] ICA: Immunochromatographic assay.

immunoassay by aid of competing antigen AFB_1-BSA and HPLC techniques (Table 1), and the commercial AFB_1 ELISA kits.[23] The high performance of the immunosensor can be explained by the synergetic coupling of Nb and nanocarbon. On one hand, as discussed in Figure 3, the GO-PB-$PTCNH_2$ served as both an excellent electrochemical probe and substrate for further conjugating abundant Nb70, which was favor of improving the sensitity of the proposed sensor. On the other hand, considering that the AFB_1 was a small molecule, the electrochemical signal variation resulted from the immune reaction between AFB_1 and Nb70 would be more noticeable than that between AFB_1 and mAb, since the molecular size of Nb70 was much smaller than that of mAb (around 1/10).

The selectivity of the immunosensor was evaluated by comparing the response of the immunosensor to Aflatoxin G_1 (AFG_1), Aflatoxin B_2 (AFB_2) and AFB_1 with a concentration of 100 $ng \cdot mL^{-1}$ for each. As shown in Figure 4d, the current response for AFB_1 was 5 times larger than that for AFB_2 and 10 times for that of AFG_1. An obvious increase in the response was observed for AFB_1 compared with those for AFG_1 and AFB_2. In addition, the current obtained from the interference can be ignored compared to that of 100 $ng \cdot mL^{-1}$ AFB_1, indicating that these interfering substances could not cause obvious signal variation and the proposed immunosensor possessed a good selectivity. The high selectivity of the as-constructed immunosensor could be ascribed to the specific interaction between AFB_1 and Nb immobilized on the electrode.

Table 2. Recovery tests of AFB_1 from real agricultural samples (n=3).

Sample	Added ($ng \cdot mL^{-1}$)	Found ($ng \cdot mL^{-1}$)	Recovery	RSD (%)
Wheat 1	0.01	0.01013	101.3	4.596
Wheat 2	1	1.067	106.7	7.783
Wheat 3	100	93.27	93.27	7.130

The stability of the prepared biosensors was examined by measuring the current response variety of immunosensors after keeping for a certain period. After the incubation of AFB_1, the immunosensors were immersed in 100 μL of PBS and stored at 4 °C in dark for 15 days. The current of immunosensors still kept 87.8% (n=5) of its initial response, which implied the perfect stability. To evaluate the reproducibility of this immunosensor, the DPVs of three different electrodes in the present of 100 $ng \cdot mL^{-1}$ AFB_1 was estimated under the same conditions. The biosensor showed a relative standard deviation (RSD) of 6.62% inter-assay and 5.66% intra-assay respectively, indicating that the immunosensor had good reproducibility.

In order to evaluate the applicability, the prepared immunosensor was applied to detect the small AFB_1 molecule in real samples which were bought from local supermarket and prepared according to our previous report [24]. The wheat samples were spiked with 0.01, 1 and 100 $ng \cdot mL^{-1}$ of AFB_1, respectively, and were detected by the proposed immunosensor. The recoveries of the spiked samples were in the range of 93.27-106.70%, with the RSD less than 7.783% (Table 2), proving that the proposed immunosensor had the potential to be used for the detection of AFB1 in real samples.

Conclusions

In summary, a direct non-competitive electrochemical immunoassay was constructed for small molecules (e.g., AFB_1) by coupling nanocarbon and Nb. On one hand, the Nb served as recognition units instead of conventional mAb. Owing to the unique properties of Nb, the non-competitive immunoassay for AFB_1 by using Nb not only avoided the extra use of the AFB_1-BSA as a competitive antigen, but also increased the assay sensitivity. On the other hand, the π-π* stacked nanocarbon assembly consisted of graphene oxide, prussian blue, and perylene derivative, not only provided abundant binding sites for Nb anchoring but also served as an excellent electrochemical probe due to promoted electron communication. Compared with the immunosensor using traditional mAb, the one prepared by synergetic coupling of Nb and nanocarbon in this work possessed two orders of magnitudes wider linear range and 10-fold more sensitivity for the determination of AFB_1 with the advantages of good reproducibility and high stability, and can be used for the quantitative determination of AFB_1 in real agriproducts. This work will open a new avenue for the direct non-competitive immunoassay of small molecules by applying the newly developed Nb as recognition units in the field of food safety.

10.1002/chem.201801202

Experimental Section

Materials and reagents

AFB_1, AFB_1-BSA and Anti-AFB_1 mAb were purchased from YouLong Bio. Co Ltd (Shanghai, China). Freund's complete adjuvant, Freund's incomplete adjuvant, anti-mouse IgG-alkaline phosphatase, isopropyl β-D-1-thiogalactopyrano-side (IPTG), Ni-NTA super flow sepharose columns, Bis (p-nitrophenyl) phosphate, Gold(III) chloride trihydrate ($HAuCl_4 \cdot 3H_2O$), ethylenediamine and BSA were purchased from Sigma-Aldrich (USA). Ficoll-Paque™ PLUS was obtained from GE Healthcare (USA). Fast Track 2.0 Kit was provided by Invitrogen (USA). The mouse anti-HA tag antibody was purchased from Covance (USA). *Pst* I, *Not* I, and T4 DNA ligase were obtained from NEB (USA). VCSM13 helper phages, TG1 cells, WK6 cells were obtained from Prof. Serge Muyldermans's lab (Laboratory of Cellular and Molecular Immunology, Vrije Universiteit Brussel, Belgium). Potassium ferricyanide ($K_3[Fe(CN)_6]$), potassium ferrocyanide ($K_4[Fe(CN)_6]$) and potassium chloride (KCl) were purchased from Shanghai Lingfeng Chemical Reagent Co., Ltd., China. 3,4,9,10-perylenetetracarboxylicdianhydride (PTCDA) was purchased from J&K Chemical Technology Co., Ltd., China. Trisodium citrate hydrate ($C_6H_5O_7Na_3 \cdot 2H_2O$) and PBS were purchased from Sangon Biotech, Shanghai, China. Iron(III) chloride hexahydrate ($FeCl_3 \cdot 6H_2O$) was obtained from Sinopharm Chemical Reagent Co., Ltd., Shanghai, China. AFB_2 and AFG_1 were purchased from Fermentek Ltd, Israel. Graphene oxide (GO) was prepared by a modified Hummers' method from natural graphite.[25] All the aqueous solutions were prepared with Milli-Q water from a Millipore water purification system (18.2 MΩ·cm). All other chemical reagents are analytical reagents grade and used directly without further purification unless otherwise specified.

Cyclic voltammetry (CV) and differential pulse voltammetry (DPV) were performed on a CHI 660e electrochemical workstation (CHI, USA) with a three-electrode system. The electrode system contained a modified GCE (3 mm in diameter), a Pt wire counter electrode, and a Ag/AgCl reference electrode (3 M KCl). DPV parameters were performed in 0.1 M PBS (pH 6.0) with 50 mV pulse amplitude, 50 ms pulse width, 0.5 s pulse period, and voltage range from −0.2 V to 0.4 V. Concentration measurements of mRNA, DNA and protein were carried out with Nano Drop 2000 (Thermos Scientific, USA). UV−Vis absorption spectra were collected from a Cary100 UV−Vis spectrophotometer (Agilent, Singapore). Scanning electron microscope (SEM) images were obtained from Zeiss Ultra Plus (Germany).

Identification of anti-AFB_1 nanobody

To obtain anti-AFB_1 Nb, an immunized phage library against AFB_1 was constructed according to our previous works by six times immunization of camel with AFB_1-BSA.[24,26] All camel experiments were conducted according to guidelines approved by the Institutional Animal Care and Use Committee of Southeast University. Afterwards, biopanning for the selection of AFB_1-specific Nb was conducted base on phage display technique. The phage display library was grown in 2× TY medium (Tryptone and yeast extract containing 100 μg·mL^{-1} ampicillin and 2% glucose) and infected with VCSM13 helper phage incubating for 30 min at room temperature. The culture was centrifuged and the supernatant was removed. The pellet was resuspended in 2 × TY medium and cultured overnight at 37 °C to get the enriched phage library. Then, the library was subjected to the selection on antigen-coated microtiter plate (20 μg AFB_1-BSA per well) as described in our previous works,[24,26] with 20 μg BSA in coating buffer as negative control. After eluted from the antigen-coated and negative wells, the phage particles were serially diluted and used to infect the TG1 *Escherichia coli (E. coli)* cells which were in exponential growth. The relative enrichment of each biopanning round was determined by counting the number of colonies grown on the square Petri dishes. In total, 95 independent colonies from each enriched round were randomly picked and analyzed by periplasmic extraction enzyme-linked immnosorbent assay (PE-ELISA). Eventually, three AFB_1-specific VHHs named Nb30, Nb33 and Nb70 were confirmed by sequencing of the positive colonies due to the different of complementarity determining region (CDR)3.

The recombinant phagemid of the positive colonies with different amino acid sequences were transformed into *E. coli* WK6 cells. For expression, the WK6 cells carrying the Nb70 expression plasmid were cultured in 330 mL terrific broth (TB) and induced by 1 mM IPTG. Immobilized metal affinity chromatography (IMAC) by using of Ni-NTA super flow sepharose columns was applied for Nbs purification because of the 6× His-tag structure of Nbs. The expression and purification procedures were performed according to our previous study.[24,26] The purity of the three Nbs were assessed by 15% sodium dodecyl sulfate-polyacrylamide gel electrophoresis (SDS-PAGE), and the molecular mass and theoretical pI is calculated using the ExPASy ProtParam Tool.[27]

Stability of anti-AFB_1 nanobody

To compare the performance of Nb70 and mAb against AFB_1 in the presence of different temperatures and organic solvents, Nb70 and mAb were diluted to 1 mg·mL^{-1} in PBS and incubated in thermo-controlled water-bath with temperature of 20 °C, 50 °C, 65 °C, 80 °C and 90 °C for 10 min, and incubated in thermo-controlled water-bath at 90 °C for 10 min, 20 min, 30 min, 40 min, 50 min and 60 min. After the treatment, each sample (5 μg·mL^{-1}) was tested for the direct binding to AFB_1-BSA (2 μg·mL^{-1}). The immunoreactions were detected by adding 100 μL of mouse anti-HA tag antibody (1:2000 dilution in PBS) and 100 μL of anti-mouse IgG-alkaline phosphatase (1:2000 dilution in PBS) for Nb70, and 100 μL of anti-mouse IgG-alkaline phosphatase (1:2000 dilution in PBS) for mAb, respectively. At last, 100 μL of phosphatase substrate was added. The absorbance at 405 nm was recorded after reaction. All the experiments were performed in triplicate.

Since MeOH, acetone, EtOH and DMSO were used in the extraction procedures of AFB_1, hence, these four organic solvents were chosen to evaluate the effect of organic-solvents on the stability of Nb70 and mAb. Briefly, AFB_1-BSA was diluted with coating buffer, and planted onto 96-well plates at 4 °C overnight. Next, 1wt% BSA (dissolved in 1× PBS) were added to the wells after being washed by PBST for blocking. After the blocking buffer was removed, the Nb70 and mAb, which were diluted by different organic solvents with the final volume ratio of each organic solvent and total solution as 10%, 20%, 30%, 40% and 50%, respectively, were added to 96-well plates and incubated for 1 h. After washing the 96-well plates with PBST, the following ELISA steps were performed according to the thermo-sensitive assay. The absorption at 405 nm was recorded finally. All the experiments were performed in triplicate.

Synthesis of GO-PB-$PTCNH_2$ nanocomposite and AuNPs

Prussian blue (PB)-functionalized GO (GO-PB) was prepared by a one-step procedure. Briefly, 5.08 mg GO was dissolved in 7.50 mL of ultrapure water, then the mixture of $FeCl_3 \cdot 6H_2O$, $K_3[Fe(CN)_6]$ and KCl were added with a mass ratio of GO: $FeCl_3 \cdot 6H_2O$: $K_3[Fe(CN)_6]$: KCl at 2.54:1:1.24:27.96, followed by an addition of 0.038 mL HCl (2 M). Finally, the GO-PB was obtained after stirring the solution at room temperature for 12 h until the mixture was dark cyan and homogeneously dispersed. To synthesize $PTCNH_2$, 1 g of PTCDA was dissolved in 5 mL acetone, added dropwise to 10 mL of ethylenediamine, and the mixture was stirred at room temperature for 40 min followed by centrifugation. Thus, the $PTCNH_2$ was obtained by washing the precipitate with ethanol and deionized water, respectively, and drying at room temperature. After that, 5.08 mg $PTCNH_2$ (with a mass ratio of $PTCNH_2$: GO at 1:1) was added to the as-obtained GO-PB dispersion (10.59 mg·mL^{-1}) and stirred at room temperature for 12 h to obtain a dark red suspension solution. The as-obtained GO-PB-

$PTCNH_2$ suspension (15.67 mg·mL^{-1}) was stored in dark at room temperature.

Gold nanoparticles (AuNPs) were synthesized according to the previous report.[28] Briefly, 0.5 mL $HAuCl_4$ solution (1 wt%) was added into 50 mL ultrapure water, and heated to 95 °C under stirring. Then, 1.25 mL of $C_6H_5O_7Na_3$ solution (1 wt%) was added into above solution, and kept boiling for 15 min under stirring until the color turned to purple. Finally, the mixture was cooled to room temperature under stirring. The as-obtained Au NPs (0.05 mg·mL^{-1}) suspension was stored at 4 °C for further use.

Preparation of Immunosensor

The process for the immunosensor fabrication was shown in Figure 1. Prior to modification, the bare glassy carbon electrode (GCE) was polished with 0.3 and 0.05 μm alumina powder, washed ultrasonically for 5 min in ultrapure water and ethanol in turn, and then dried at room temperature. 10 μL of the GO-PB-$PTCNH_2$ suspension was then dropped onto the GCE and dried at room temperature for 24 h. Afterwards, the AuNPs was assembled on the above electrode by dipping the modified GCE in AuNPs solution for 3 h at room temperature. Next, Nb70 was further immobilized onto the modified electrode through the electrostatic interaction between Nb70 and AuNPs by dropping 6 μL of Nb70 (2.0 mg·mL^{-1}) in 0.1 M PBS onto the modified GCE and kept for 2 h at room temperature. Then the electrode was washed with 0.1 M PBS and blocked by 6 μL of 0.5 wt% BSA solution (in 0.1 M PBS) at room temperature for 30 min to block the nonspecific binding sites. Finally, 10 μL of AFB_1 with various concentrations were added to the electrode and incubated for 2 h at room temperature. The as-fabricated immunosensor was stored in 0.1 M PBS at 4 °C for further use.

Preparation of spiked wheat samples for reliability evaluation

The spiked samples were prepared by spiking AFB_1 into wheat samples. Briefly, 10 mL of the protein extraction solution (0.1 M PBS containing 0.1% BSA and 0.05% Tween-20) was added into 1 g of the dried and homogenized wheat powder samples. After a gentle shaking at room temperature for 2 h, the suspensions were centrifuged at 10000 g for 10 min. Afterwards, the supernatant was diluted 1000 folds by 0.1 M PBS to reduce the viscosity and matrix effect of the extracts, and then spiked with AFB_1 with three different concentrations (0.01, 1, and 100 ng•mL^{-1}). The mixed extracts were used for sample analysis by the constructed electrochemical immunoassay, and each spiked sample was analyzed with three sets of parallel control. The final concentration of spiked samples was determined by the interpolation method according to the standard calibration plot.

Conflicts of interest Conclusions

There are no conflicts to declare.

Acknowledgements

This work is supported by the National Natural Science Foundation of China (21675022 and 21775018) and Program from the Natural Science Foundation of Jiangsu Province (BK20170084 and BK20160028).

Keywords: direct immunoassay, nanobody, electrochemical, prussian blue, AFB_1

[1] a) P. W. Christopher; M. Ruggero. *Science* **2008**, *322*, 1464-1465; b) R. E. Minto; C. A. Townsend. *Chem. Rev.* **1997**, *97*, 2537-2556; c) G. S. Shephard. *Chem. Soc. Rev.* **2008**, *37*, 2468.

[2] P. Li; Q. Zhang; W. Zhang. *Trends Anal. Chem.* **2009**, *28*, 1115-1126.

[3] IARC "Some Naturally Occurring Substances Food Items and Constituents, Heterocyclic Aromatic Amines and Mycotoxins," IARC, 1993.

[4] a) K. Schulze; S. Imbeaud; E. Letouzé; L. B. Alexandrov; J. Calderaro; S. Rebouissou; G. Couchy; C. Meiller; J. Shinde; F. Soysouvanh; A.-L. Calatayud; R. Pinyol; L. Pelletier; C. Balabaud; A. Laurent; J.-F. Blanc; V. Mazzaferro; F. Calvo; A. Villanueva; J.-C. Nault; P. Bioulac-Sage; M. R. Stratton; J. M. Llovet; J. Zucman-Rossi. *Nat. Genet.* **2015**, *47*, 505-511; b) J. M. Crawford; T. P. Korman; J. W. Labonte; A. L. Vagstad; E. A. Hill; O. Kamari-Bidkorpeh; S.-C. Tsai; C. A. Townsend. *Nature* **2009**, *461*, 1139-1143.

[5] Y. Lin; Q. Zhou; D. Tang; R. Niessner; D. Knopp. *Anal. Chem.* **2017**, *89*, 5637-5645.

[6] a) Y. Lin; Q. Zhou; D. Tang; R. Niessner; H. Yang; D. Knopp. *Anal. Chem.* **2016**, *88*, 7858-7866; b) X. Wang; R. Niessner; D. Knopp. *Analyst* **2015**, *140*, 1453-1458; c) T. He; Y. Wang; P. Li; Q. Zhang; J. Lei; Z. Zhang; X. Ding; H. Zhou; W. Zhang. *Anal. Chem.* **2014**, *86*, 8873-8880; d) X. Tang; P. Li; Q. Zhang; Z. Zhang; W. Zhang; J. Jiang. *Anal. Chem.* **2017**, *89*, 11520–11528; e) X. Wang; R. Niessner; D. Tang; D. Knopp. *Anal. Chim. Acta* **2016**, *912*, 10-23.

[7] T. Fang; J. N. Duarte; J. Ling; Z. Li; J. S. Guzman; H. L. Ploegh. *Angew. Chem. Int. Ed* **2016**, *55*, 2416-2420; *Angew. Chem.* **2016**, *128*, 2462-2466.

[8] H. Wang; G. Li; Y. Zhang; M. Zhu; H. Ma; B. Du; Q. Wei; Y. Wan. *Anal. Chem.* **2015**, *87*, 11209-11214.

[9] M. Zhang; C. Hou; A. Halder; J. Ulstrup; Q. Chi. *Biosens. Bioelectron.* **2017**, *89*, 570-577.

[10] a) V. Georgakilas; J. N. Tiwari; K. C. Kemp; J. A. Perman; A. B. Bourlinos; K. S. Kim; R. Zboril. *Chem. Rev.* **2016**, *116*, 5464-5519; b) Y. Guo; X. Jia; S. Zhang. *Chem. Commun.* **2011**, *47*, 725-727.

[11] B. Kong; X. Sun; C. Selomulya; J. Tang; G. Zheng; Y. Wang; D. Zhao. *Chem. Sci.* **2015**, *6*, 4029-4034.

[12] a) Y.-M. Lei; W.-X. Huang; M. Zhao; Y.-Q. Chai; R. Yuan; Y. Zhuo. *Anal. Chem.* **2015**, *87*, 7787-7794; b) L. Gao; J. He; W. Xu; J. Zhang; J. Hui; Y. Guo; W. Li; C. Yu. *Biosens. Bioelectron.* **2014**, *62*, 79-83; c) Y. Pan; W. Shan; H. Fang; M. Guo; Z. Nie; Y. Huang; S. Yao. *Biosens. Bioelectron.* **2014**, *52*, 62-68.

[13] Y. Zhang; Y. Wen; Y. Liu; D. Li; J. Li. *Electrochem. Commun.* **2004**, *6*, 1180-1184.

[14] Q. Chen; C. Yu; R. Gao; L. Gao; Q. Li; G. Yuan; J. He. *Biosens. Bioelectron.* **2016**, *79*, 364-370.

[15] H. Ma; J. Sun; Y. Zhang; C. Bian; S. Xia; T. Zhen. *Biosens. Bioelectron.* **2016**, *80*, 222-229.

[16] X. Xu; X. Liu; Y. Li; Y. Ying. *Biosens. Bioelectron.* **2013**, *47*, 361-367.

[17] Y. Nonaka; K. Saito; N. Hanioka; S. Narimatsu; H. Kataoka. *J. Chromatogr. A* **2009**, *1216*, 4416-4422.

[18] W.-B. Shim; M. J. Kim; H. Mun; M.-G. Kim. *Biosens. Bioelectron.* **2014**, *62*, 288-294.

[19] Z. Hu; W. P. Lustig; J. Zhang; C. Zheng; H. Wang; S. J. Teat; Q. Gong; N. D. Rudd; J. Li. *J. Am. Chem. Soc.* **2015**, *137*, 16209-16215.

[20] D. Tang; B. Liu; R. Niessner; P. Li; D. Knopp. *Anal. Chem.* **2013**, *85*, 10589-10596.

[21] D. Saha; D. Acharya; D. Roy; D. Shrestha; T. K. Dhar. *Anal. Chim. Acta* **2007**, *584*, 343-349.

[22] X. Li; P. Li; Q. Zhang; R. Li; W. Zhang; Z. Zhang; X. Ding; X. Tang. *Biosens. Bioelectron.* **2013**, *49*, 426-432.

[23] a) https://www.biovision.com/aflatoxin-b1-afb1-elisa-kit.html; b) https://www.mybiosource.com/prods/ELISA-Kit/Aflatoxin-B1/AFB1/datasheet.php?products_id=280406.

[24] Q. Zhou; G. Li; Y. Zhang; M. Zhu; Y. Wan; Y. Shen. *Anal. Chem.* **2016**, *88*, 9830-9836.

[25] Y. Zhang; K. Fugane; T. Mori; L. Niu; J. Ye. *J. Mater. Chem.* **2012**, *22*, 6575.

[26] G. Li; M. Zhu; L. Ma; J. Yan; X. Lu; Y. Shen; Y. Wan. *ACS Appl. Mater. Interfaces* **2016**, *8*, 13830-13839.

[27] C. Achmuller; W. Kaar; K. Ahrer; P. Wechner; R. Hahn; F. Werther; H. Schmidinger; M. Cserjan-Puschmann; F. Clementschitsch; G. Striedner; K. Bayer; A. Jungbauer; B. Auer. *Nat. Methods* **2007**, *4*, 1037-1043.

[28] J.-W. Park; J. S. Shumaker-Parry. *ACS Nano* **2015**, *9*, 1665-1682.

10.1002/chem.201801202

WILEY-VCH

FULL PAPER

Text for Table of Contents

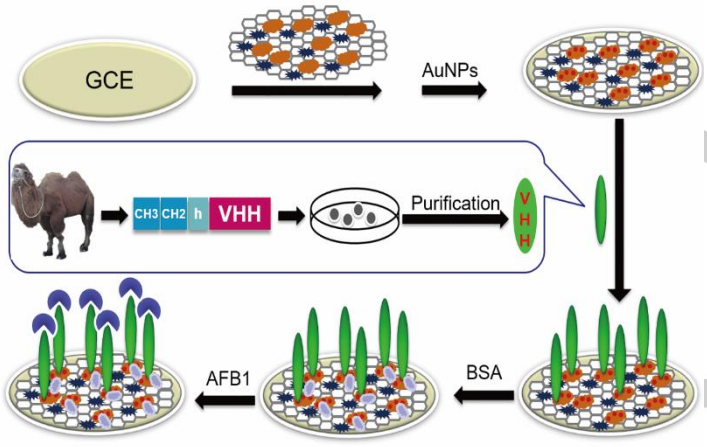

Deng Pan, Guanghui Li, Huizhen Hu, Mingming Zhang, Huaijia Xue, Min Zhu, Xue Gong, Yuanjian Zhang, Yakun Wan and Yanfei Shen**